Regional Wall Thickening of Left Ventricle Evaluated by Gated Positron Emission Tomography in Relation to Myocardial Perfusion and Glucose Metabolism

Keiji Yamashita, Nagara Tamaki, Yoshiharu Yonekura, Hiroshi Ohtani, Yasuhiro Magata, Ryuji Nohara, Hirofumi Kambara, Chuichi Kawai, Toshihiko Ban, and Junji Konishi

Department of Radiology and Nuclear Medicine, Third Division, Department of Internal Medicine, Department of Cardiovascular Surgery, Kyoto University, School of Medicine, Kyoto, Japan

Regional wall thickening was assessed by electrocardiographically gated positron emission tomography (ECG-gated PET) in 26 patients with coronary artery disease. The standardized percent count increase from end-diastole to end-systole (S-percent CI) was calculated as an index of wall thickening. The S-percent CI was 77.8% ± 28.9% in the segments with normal perfusion at rest, 51.9% ± 29.5% in those with mild hypoperfusion, and 32.8% ± 30.9% in those with severe hypoperfusion (p < 0.001, each). Among the segments with resting hypoperfusion, the S-percent CI was 38.9% ± 31.5% in those without stress-induced ischemia and 48.7% ± 30.9% in those with ischemia (p < 0.05). Furthermore, among resting severe hypoperfusion, the S-percent CI was 23.0% ± 23.9% in the segments without fluorine-18-fluorodeoxyglucose (FDG) uptake and 37.8 ± 32.9% in those with FDG uptake (p < 0.05). These results suggest that stress-induced ischemia and FDG accumulation correlated with wall thickening. Thus, quantitative analysis of regional wall thickening seems to be useful for combined analysis of regional function, perfusion and metabolism in coronary patients.

J Nucl Med 1991; 32:679–685

Positron emission tomography (PET) is an excellent means for assessing regional blood flow and metabolism in vivo. In heart studies, PET has been used for the detection of myocardial ischemia (1–8), identification of tissue viability (1,5,9–12), and pathophysiologic assessment of various myocardial diseases (13). Recently, electrocardiographically (ECG) gated acquisition has become available (14).

We previously reported that the percent count increase of the left ventricle (LV) by ECG-gated PET could be used as an index of regional wall thickening in normal persons and patients with coronary artery disease (CAD) (15).

In this study we have analyzed the correlation of wall thickening, resting and stress myocardial perfusion, and myocardial metabolism of fluorine-18-fluorodeoxyglucose (FDG) using ECG-gated PET.

SUBJECTS AND METHODS

Normal Control and Patient Population

Nine healthy volunteers were selected as normal controls. They were all men (age range: 31–70 yr, mean 52.3) with normal blood pressure, no abnormality on ECG, no cardiac symptoms, nor other medical problems.

Twenty-six clinically stable patients with CAD (all men), aged 48–64 yr (mean 58.0) were selected for this study. Twenty-three patients had myocardial infarction (MI) and three patients had angina pectoris. Location of MI was documented with ECG findings (Table 1). Electrocardiographic location of infarction was based on the development of significant Q-waves (>0.03 ms) in leads V_1-V_2 (anteroseptal), V_3-V_4 (anterior), V_5-V_6 (anterolateral), I, aVL and V_1-V_6 (extensive anterior), II, III and aVF (inferior), II, III, aVF and V_1 (inferoposterior), and V_1 and V_{5-6} (posterolateral) (16). Eight patients had anterior wall MI, four had anteroseptal wall MI, six had extensive anterior wall MI, four had inferior wall MI, one had an inferoposterior wall MI, and one had anterolateral wall infarctions (MI was seen at two regions in one patient). One patient had non-Q wave infarction with significant evolution of ST segment or T-wave changes. The interval from the onset of MI ranged from 1 mo to 10 yr (mean 20.8 mo). All of the patients gave written informed consent. Twenty-five patients had significant coronary artery stenosis (≥75% stenosis) on coronary arteriography but one patient had no significant stenosis. Those with marked LV hypertrophy on ECG or echocardiography were excluded in this analysis.

ECG-gated and Static PET with ^{13}N-ammonia and FDG

As reported previously (15), PET was performed using a whole-body, multi-slice PET scanner (PositologicalII; Hitachi Medical Corp., Tokyo) (17). The effective resolution on a reconstructed image (128 × 128 matrix) with a Shepp-Logan filter convoluted

TABLE 1
Patient List

Patient	Age (y.o)	Sex	Site of MI	Interval from MI	Coronary artery stenosis (≥75%)	Wall motion* abnormality	Stress ischemia	[18F]FDG accumulation
1	64	M	AP	—	3VD	Sep	—	Lat
2	56	M	AP	—	3VD	Sep, Ant, Lat	Ant, Sep, Lat	—
3	64	M	AP	—	3VD	—	Ant, Lat	—
4	60	M	Ant	8 yr	3VD	Sep, Ant, Lat	—	Ant, Lat
5	55	M	Ant	5 mo	LAD, CX	Sep, Ant, Lat	Sep, Ant	Ant
6	55	M	Ant	2 mo	LAD, CX	Sep, Ant	Sep, Ant	Ant
7	59	M	Ant	9 mo	LAD	Sep, Ant	Sep, Ant	Sep, Ant, Lat
8	60	M	Ant	8 yr	3VD	Sep, Ant, Lat	—	Ant, Lat
9	60	M	Ant	2 mo	LAD	Ant, Lat	—	Ant, Lat
10	62	M	Ant	8 mo	LAD, CX	Sep, Ant	Sep, Ant	Sep, Ant, Lat
11	53	M	Ant-Sep	5 mo	LAD, CX	—	Ant	Sep, Lat
12	59	M	Ant-Sep	6 mo	LAD	Sep, Ant	Sep, Ant	Sep, Ant
13	58	M	Ant-Sep	9 mo	LAD, CX	Ant, Lat	Ant, Lat	Ant, Lat
14	58	M	Ant-Sep	5 mo	LAD, CX	Sep, Ant, Lat	Ant, Lat	Sep, Ant, Lat
15	60	M	Ant, Inf	1 yr	no significant stenosis	Ant	—	—
16	55	M	ext-Ant	2 mo	LAD	Sep, Ant, Lat	—	—
17	58	M	ext-Ant	1 yr	3VD	Sep, Ant, Lat	Lat	Sep, Lat
18	48	M	ext-Ant	10 yr	3VD	Sep, Ant, Lat	Ant, Lat	Ant, Lat
19	58	M	ext-Ant	1.4 yr	3VD	Sep, Ant, Lat	Sep, Ant	Sep, Ant
20	61	M	ext-Ant	2.7 yr	3VD	Sep, Ant, Lat	Ant, Lat	Ant, Lat
21	61	M	ext-Ant	2 yr	3VD	Sep, Ant, Lat	Ant, Lat	Ant, Lat
22	58	M	Inf	4 mo	3VD	Sep	Lat	Lat
23	56	M	Inf	1.5 yr	RCA, LAD	Ant, Lat	Sep, Ant, Lat	Lat
24	56	M	Inf	1.7 yr	RCA, LAD	Sep, Ant	Ant, Lat	Ant, Lat
25	58	M	Inf-Post	1.2 yr	RCA, CX	Lat	Sep, Lat	Lat
26	55	M	Ant-Lat (non-Q)	1 mo	CX	Sep, Lat	Ant, Lat	Lat

MI = myocardial infarction; AP = angina pectoris; Ant = anterior wall; Sep = septal wall; Inf = inferior wall; ext = extensive; Post-posterior wall; Lat = lateral wall; non-Q = non-Q wave infarction; 3VD = three vessels disease; LAD = left anterior descending artery; CX = circumflex artery; RCA = right coronary artery

* Evaluated by ECG-gated PET; the S-percent count increase <60% was regarded as wall motion abnormality. Inferior and posterior wall were excluded for evaluation

with 2 mm sigma Gaussian was approximately 9 mm in FWHM (*17*).

A small cyclotron (SYPRIS 325; Sumitomo Heavy Industry, Tokyo) was used for production of ^{13}N-ammonia and FDG. Nitrogen-13-ammonia was produced by ^{16}O(p, α) ^{13}N nuclear reaction with water irradiation, followed by a reduction to ^{13}N-ammonia with titanous hydroxide (*6,7*). The ^{18}F was produced by ^{20}Ne(d, α) ^{18}F nuclear reaction and ^{18}F-labeled 2-fluoro-2-deoxy-D-glucose (FDG) was synthesized by the acetyl hypofluorite method.

Following a 15-min transmission scan for accurate correction of attenuation, a resting perfusion scan was recorded for 3–5 min beginning 3 min after i.v. injection of 370–740 MBq (10–20 mCi) of ^{13}N-ammonia. An ECG-gated scan was recorded immediately after the static scan for 1000–1200 beats (15–20 min). Seven transverse slices of the left ventricle at end-diastole (ED) and end-systole (ES) were obtained with a slice spacing of 16 mm. Two hours later, graded exercise was performed using a supine ergometer attached to the PET camera bed (*7,18,19*). The exercise continued until the patient had fatigue, severe chest pain, dyspnea, more than 0.2 mV of ST-segment depression, or 85% of the age-predicted maximal heart rate (*7,19*). Another dose of ^{13}N-ammonia was injected at peak exercise and the exercise was

continued another 30–60 sec. The exercise perfusion scan was performed 3 min after tracer injection. Two scans were performed to obtain interpolated positron images (consequently 14 contiguous slices of the myocardium with an 8-mm interval).

The FDG scan was performed separately within a week after the ^{13}N-ammonia perfusion study. All patients fasted for at least 5 hr before the study. Seventy-four to 254 MBq (2 to 7 mCi) of FDG were injected at rest. Two emission scans were recorded 60 min after injection for 8 min each and 14 contiguous slices were obtained with 8-mm intervals (*20*).

Analysis of ECG-gated PET

Two experienced observers analyzed ECG-gated PET twice. As reported previously (*15*), three slices were selected for analysis from seven transverse sections of LV myocardium with 16-mm intervals using ^{13}N-ammonia. When the LV lumen was not seen clearly, such slices were excluded (in normal controls, 3 of 9 upper slices were excluded; in patients with CAD, 3 of 26 upper slices and 9 of 26 lower slices were excluded). The matrices of these images were reduced from 128 × 128 into 64 × 64 matrices (matrix size was 5 × 5 mm). The LV wall was divided into 12 segments at every 30°. Eight segments from septal, anterior to lateral wall (numbered in order) were analyzed (*15*). The ED and

TABLE 2

The Percent Count Increase in Normal Controls (%)

Slice/Segment	1	2	3	4	5	6	7	8
Upper slice	39.8 ± 10.1	41.5 ± 7.5	49.5 ± 13.7	51.7 ± 12.6	45.5 ± 18.1	46.2 ± 10.4	59.3 ± 16.1	72.8 ± 26.5
Middle slice	39.8 ± 12.9	42.4 ± 11.4	49.6 ± 16.1	62.1 ± 13.6	50.9 ± 13.9	53.3 ± 16.1	61.3 ± 15.0	66.1 ± 17.2
Lower slice	32.9 ± 7.2	44.7 ± 9.6	47.9 ± 11.9	72.6 ± 21.4	56.0 ± 16.5	48.7 ± 15.0	44.7 ± 17.0	57.2 ± 16.7
Posterior wall	Post-1	Post-2						
	51.4 ± 10.9	58.9 ± 20.2						

Segments are numbered in order from septal (1, 2), anterior (4, 5) to lateral wall (7, 8). When posterior wall is clearly seen, it is also analyzed (numbered P1, P2). Values are mean ± s.d.

ES count in each segment was calculated using five-point averaging circumferential profile analysis (15).

In the normal controls, the percent count increase (percent CI) was calculated in each segment as follows:

$$\text{percent CI} = \frac{\text{ES count} - \text{ED count}}{\text{ED count}} \times 100(\%)$$

(Normal values of the percent CI are given by Table 2).

In patients with CAD, the standardized percent count increase (S-percent CI) was calculated as follows:

$$\text{S-percent CI} = \frac{\text{percent CI}}{\text{normal value of each seg.}} \times 100(\%).$$

Analysis of Perfusion Images

Regional myocardial perfusion was semiquantitatively assessed by circumferential profile analysis of ^{13}N-ammonia. The circumferential profile curve of each segment was compared with the lower limit of normal value at each segment which was determined as mean minus two standard deviations of the 12 normal subjects (18,21). The segments with perfusion below the lower limit were considered as hypoperfusion. Among hypoperfusion, those below the lower limit minus 10% on the profile curve at each slice were defined as severe hypoperfusion and those equal or over the lower limit minus 10% on the profile curve were defined as mild hypoperfusion.

Resting and stress perfusion were compared on the circumferential profile curves (maximum of 100% each). The segments with the stress perfusion ≤ 10% below the resting perfusion were defined as those with stress-induced ischemia. Those with the stress perfusion > 10% below the resting perfusion were defined as no ischemia (18,19).

Analysis of FDG Accumulation

Among the segments with hypoperfusion, FDG accumulation at rest was evaluated. The hypoperfused segments with FDG uptake more than the normal range of FDG, were defined as those with FDG uptake. The hypoperfused segments with FDG uptake less or within normal range of FDG, were defined as no FDG uptake. The normal range of FDG uptake was calculated as mean ± 2 s.d. of regional FDG uptake from five normal subjects in a fasting condition.

Statistical Analysis

Each value was expressed as mean ± standard deviation. The differences of the S-percent CI were analyzed using the student's paired t-test. The relation between stress-induced ischemia and FDG accumulation was analyzed using the Chi-square test. P

values of less than 0.05 was considered the significant level in both tests.

RESULTS

### Inter- and Intraobserver Variability in Analysis of the S-percent CI in ECG-gated PET

In normal control, inter- and intraobserver variability was 3.5% and 2.7%, respectively. In patients with CAD, inter- and intraobserver variability was 7.3% and 5.8%, respectively.

ECG-gated PET in Normal Controls

Table 2 shows the values of the percent CI in normal controls. Since the percent CI in various segments was different even in normal controls (15), the S-percent CI was calculated as an universal index of systolic wall thickening. The S-percent CI in 192 segments of 9 normal cases was 100.0% ± 26.5%.
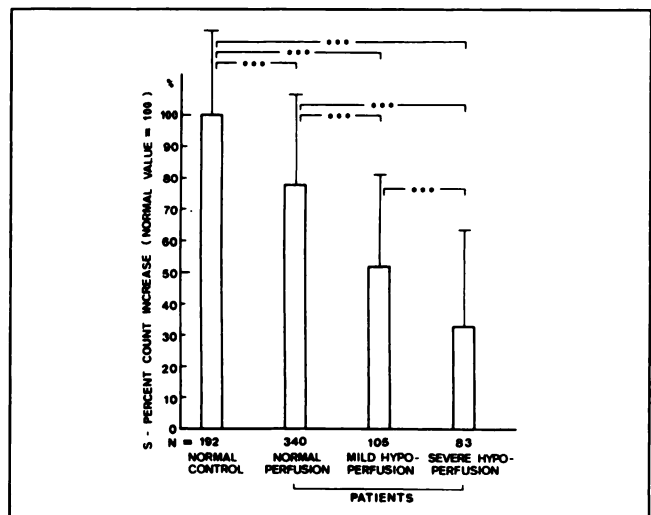
FIGURE 1. Correlation between the standardized percent count increase (S-CI) and resting perfusion are shown. The S-percent count increase decreased as decrease in resting perfusion. Note significant decrease of the S-CI in normal perfusion of coronary patients in comparison with that in normal control. Statistical probabilities were determined by the Student's paired t-test: ***: p < 0.001.
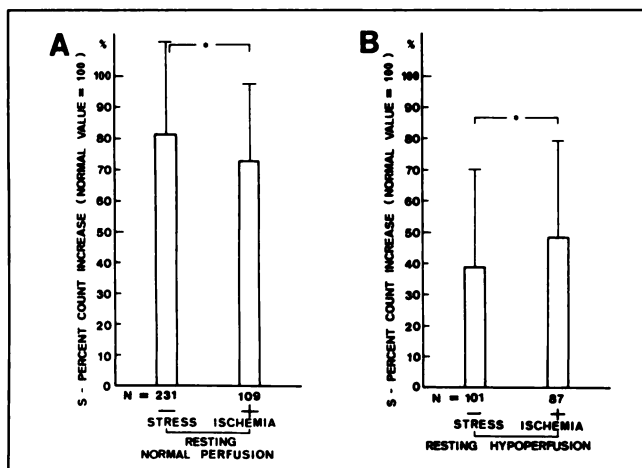
FIGURE 2. Among the segments with normal resting perfusion in coronary patients, the standardized percent count increase (S-CI) in those without stress-induced ischemia was significantly better than that in those with ischemia (A). Among the segments with resting hypoperfusion in coronary patients, the S-CI in those without stress-induced ischemia (=persistent hypoperfusion) was significantly less than that in those with stress-induced ischemia (=transient hypoperfusion) (B). Statistical probabilities were determined by the paired t-test: *: p < 0.05.

The S-percent CI Versus the Resting Perfusion

The S-percent CI was compared with resting perfusion in the patients with CAD (Fig. 1). The S-percent CI was 77.8% ± 28.9% in normal perfusion, 51.9% ± 29.5% in mild hypoperfusion, and 32.8% ± 30.9% in severe hypoperfusion. Regional wall thickening significantly decreased as resting myocardial perfusion decreased (p < 0.001). In addition, the S-percent CI in normal resting perfusion in the patients with CAD was lower than that in normal control (p < 0.001).

The S-percent CI Versus Stress-Induced Ischemia

The S-percent CI was compared with stress-induced ischemia among the segments with resting normal perfusion (Fig. 2A). The S-percent CI was significantly higher in the segments without stress-induced ischemia (80.7% ± 30.2%) than those with ischemia (72.3% ± 24.9%) (p < 0.05).

On the other hand, among the segments with resting hypoperfusion (Fig. 2B), the S-percent CI was significantly

lower in the segments without stress-induced ischemia (38.9% ± 31.5%) (Fig. 3A-B) than those with ischemia (48.7% ± 30.9%) (Fig. 4A-B) (p < 0.05).

The S-percent CI Versus FDG Accumulation

The S-percent CI was compared with FDG accumulation among the segments with resting hypoperfusion. The S-percent CI was 38.9% ± 29.9% in the segments without FDG uptake and 46.5% ± 32.3% in those with FDG uptake (p < 0.2, not significant).

When the segments with resting severe hypoperfusion were selected for analysis, the S-percent CI was significantly lower in the segments without FDG uptake (23.0% ± 23.9%) than those with FDG uptake (37.8% ± 32.9%) (p < 0.05) (Fig. 5).

Stress Ischemia Versus FDG Accumulation

Table 3 shows the correlation between stress-induced ischemia and FDG accumulation among the segments with resting hypoperfusion. FDG uptake was observed in 78 of the 87 segments with stress-induced ischemia (89.7%) (Fig. 4A) but only in 37 of the 115 segments without ischemia (32.2%) (p < 0.001) (Fig. 3B).

DISCUSSION

Our data indicate that regional wall thickening decreased as resting myocardial perfusion decreased and that this was related to the presence of stress-induced ischemia and FDG uptake.

Technical Considerations

Recently, we reported on a method for the geometrical quantitative analysis of regional wall thickening by ECG-gated PET using ^{13}N-ammonia in normal persons and patients with CAD (15). Based on the principle of partial volume effect on PET images (22,23), segments with normal wall thickening are expected to have a count increase from ED to ES, while those with decreased or no wall thickening should have decreased or no count increase. Since the values of the percent CI were significantly different among the segments in normal control, we used the S-percent CI (corrected by normal value of each segment of three slices) as an index of regional wall thickening.

We found a good correlation between the percent CI
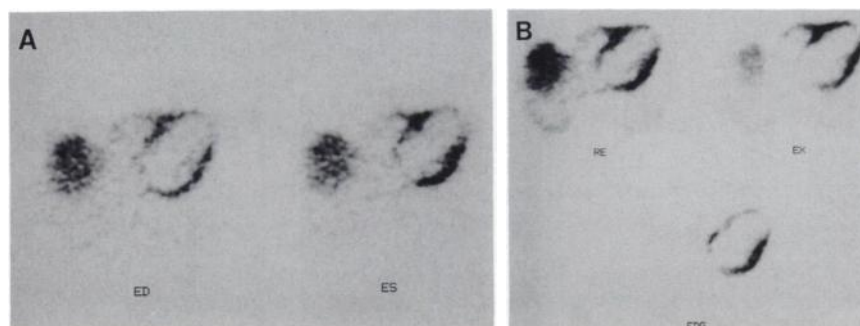
FIGURE 3. Patient 4 of Table 1 (anterior myocardial infarction). In ECG-gated PET image (A), the count increased well from end-diastole to end-systole in septum and lateral walls but did not increase in anterior wall. In the resting (RE) and exercise (EX) ^{13}N-ammonia PET image (B), persistent defect was seen in anterior wall. In the FDG image (B), FDG uptake was not seen.

FIGURE 4. Patient 18 of Table 1 (extensive anterior myocardial infarction). In the ECG-gated PET image (A), the count increased well from end-diastole to end-systole in septum and lateral wall and mildly increased in anterior wall. In the resting (RE) and exercise (EX) ^{13}N-ammonia PET image (B), the segments of anterior to lateral wall were all severe hypoperfusion with stress-induced ischemia. In the FDG image (B), FDG uptake was seen in anterior to lateral wall especially in lateral wall.
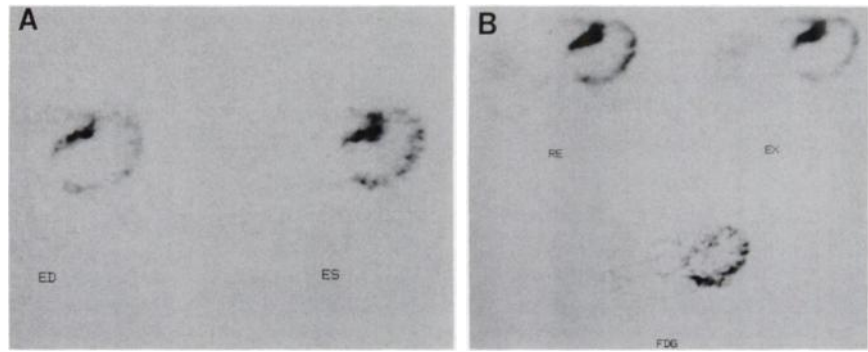
and regional wall thickening assessed by MRI and wall motion assessed by contrast left ventriculography (15). The major advantage of this technique is the ability to assess regional wall thickening in relation to perfusion and metabolism on exactly the same area.

Relation to Myocardial Perfusion

The S-percent CI significantly decreased as resting perfusion decreased. In the previous study, wall motion amplitude by two-dimensional echocardiography decreased as the wall motion score by contrast ventriculography decreased in the area of acute myocardial infarction, which seemed to reflect myocardial damage (24).

Interestingly, the S-percent CI in the segments with normal resting perfusion in the patients with CAD was significantly smaller than that in normal controls, suggesting that regional wall thickening may decrease in the patients with CAD in spite of normal resting perfusion (15). This supports our previous study in which the percent CI in the segments with normal wall motion in patients with CAD was less than that in normal controls (15). In our study, most of the patients had two- or three-vessel coronary stenosis. Therefore, segments showing decreased wall thickening in spite of normal resting perfusion may contain ischemic myocardium. This was supported by our

data showing decrease in the S-percent CI in the segments with normal resting perfusion but with stress-induced ischemia in patients with CAD. In addition this may be partly explained by the prolonged postischemic ventricular dysfunction, the so called "stunned" myocardium (25,26).

In contrast, among the segments with resting hypoperfusion, the S-percent CI in the segments with stress-induced ischemia was significantly greater than that with no stress-induced ischemia. This supports the previous study by Tamaki (27) showing that wall motion in areas of a reversible perfusion defect was significantly greater than that in an area of non-reversible defect on stress thallium-201 scans. The segments with resting hypoperfusion but with stress-induced ischemia may contain ischemic but viable myocardium, whereas those with hypoperfusion without stress-induced ischemia may contain mostly infarcted tissues without viable myocardium. These data suggest that preserved wall thickening in MI may reflect residual myocardial viability.

Relation to FDG Uptake

The segments with increased FDG uptake as a marker of exogeneous glucose utilization (1,5,28) reflected ischemic but viable myocardium (1,5,10). Since FDG was administered to patients in the fasting condition, FDG uptake was augmented in the ischemic myocardium compounds to the normal myocardium. This should not cause a significant difference of the S-percent CI between the segments with and without FDG uptake, since no FDG uptake indicates either normal or infarcted myocardium. However, when the segments with severe hypoperfusion at rest were selected for analysis, the S-percent CI in the

FIGURE 5. Among the segments with resting severe hypoperfusion in coronary patients, the standardized percent count increase in those without FDG uptake was significantly less than that in those with FDG uptake. Statistical probabilities were determined by the student's paired t-test: *: p < 0.05.
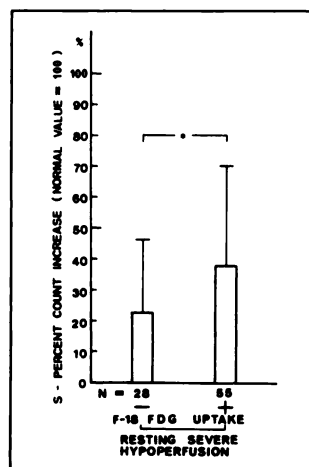
TABLE 3
Correlation Between FDG and Stress Ischemia Among Segments with Resting Hypoperfusion

	Stress ischemia (+)	Stress ischemia (−)
FDG (+)	78	37
FDG (−)	9	64
	p < 0.001	

segments with FDG uptake was significantly greater than that without FDG uptake suggesting that those with FDG uptake may reflect ischemic but viable myocardium.

Stress-induced ischemia and FDG uptake correlated well with each other. This may support our previous report showing the close correlation between stress-induced ischemia and FDG accumulation (29,30).

Limitation of This Method

The normal value of S-percent CI of each segment may be different in the dilated heart and in subjects where no LV dilatation is observed. In addition, the hypertrophic heart should not be analyzed without correction (15).

A major limitation of this method is slice sequence: it uses transverse slices. Therefore, changes in the orientation of the LV wall relative to imaging plane from ED to ES may influence the analysis of systolic count increase (31). A true three-dimensional assessment using cardiac short- and long-axis sections (32) may be needed in the future. In addition, we performed our FDG study on a separate day from the ^{13}N-ammonia perfusion study (20,27), which might be a problem in the study of out-patients. In some other institutions, however, perfusion and FDG studies have been performed on the same day (10-13).

Clinical Implications

PET is useful for the analysis of myocardial perfusion and metabolism (1-14). Previously, we reported the capability of ECG-gated PET for quantitative analysis of regional wall thickening (15). This ECG-gated acquisition PET study permits combined analysis of regional wall thickening with myocardial perfusion and metabolism on the same basis. This study documents the close relationship between regional wall thickening, myocardial perfusion, and glucose metabolism. The present study suggests that regional wall thickening decreased significantly in patients with IHD, even if the perfusion is normal, and decreased as resting myocardial perfusion decreased. In addition, regional wall thickening was significantly preserved in stress-induced ischemia and FDG accumulation zones in the segments with hypoperfusion.

ACKNOWLEDGMENTS

REFERENCES

1. Brunken R, Tillisch J, Schwaiger M, et al. Regional perfusion, glucose metabolism and wall motion in patients with chronic electrographic Q-wave infarctions: evidence for persistence of viable tissue in some infarct regions by positron emission tomography. Circulation 1986;73:951-963.
2. Schelbert HR, Phelps ME, Huang SC, et al. N-13-ammonia as an indicator of myocardial blood flow. Circulation 1981;63:1259-1272.
3. Bergmann SR, Fox KA, Rand AL, et al. Quantification of regional myocardial blood flow in vivo with H₂¹⁵O. Circulation 1984;70:724-733.
4. Gould KL, Goldstein RA, Mullani NA, et al. Noninvasive assessment of coronary stenosis by myocardial perfusion imaging during pharmacologic coronary vasodilation. VIII. Clinical feasibility of positron cardiac imaging without cyclotron using generator-produced rubidium-82. J Am Coll Cardiol 1986;7:775-789.
5. Marshall RC, Tillisch JH, Phelps ME, et al. Identification and differentiation of resting myocardial ischemia and infarction in man with positron computed tomography, ¹⁸F-labeled fluorodeoxyglucose and N-13 ammonia. Circulation 1983;67:766-778.
6. Yonekura Y, Tamaki N, Senda M, et al. Detection of coronary artery disease with ¹³N-ammonia and high-resolution positron emission computed tomography. Am Heart J 1987;113:645-654.
7. Tamaki N, Yonekura Y, Senda M, et al. Myocardial positron computed tomography with ¹³N-ammonia at rest and during exercise. Eur J Nucl Med 1985;11:246-251.
8. Goldstein RA, Kirkeeide RL, Smalling RW, et al. Changes in myocardial perfusion reserve after PTCA: noninvasive assessment with positron tomography. J Nucl Med 1987;28:1262-1267.
9. Ratib O, Phelps ME, Huang SC, Henze E, Selin CE, Schelbert HR. Positron tomography with deoxyglucose for estimating lacal myocardial glucose metabolism. J Nucl Med 1982;23:577-586.
10. Tillisch J, Brunken R, Marshall R, et al. Reversibility of cardiac wall-motion abnormalities predicted by positron tomography. N Engl J Med 1986;314:884-888.
11. Brunken R, Schwaiger M, Grover-Mckay M, Phelps ME, Tillisch J, Schelbert HR. Positron emission tomography detects tissue metabolic activity in myocardial segments with persistent thallium perfusion defects. J Am Coll Cardiol 1987;10:557-567.
12. Schwaiger M, Brunken R, Grover-Mckay M, et al. Regional myocardial metabolism in patients with acute myocardial infarction assessed by positron emission tomography. J Am Coll Cardiol 1986;8:800-808.
13. Grover-Mckay M, Schwaiger M, Krivokapich J, Perloff JK, Phelps ME, Schelbert HR. Regional myocardial blood flow and metabolism at rest mildly symptomatic patients with hypertrophic cardiomyopathy. J Am Coll Cardiol 1989;13:317-324.
14. Hoffman EJ, Phelps ME, Wisenberg G, Schelbert HR, Kuhl DE. Electrographic gating in positron emission computed tomography. J Comput Assist Tomogr 1979;3:733-739.
15. Yamashita K, Tamaki N, Yonekura Y, et al. Quantitative analysis of regional wall motion by gated myocardial positron emission tomography: validation and comparison with left ventriculography. J Nucl Med 1989;30:1775-1786.
16. The criteria committee of the New York association. Nomenclature and criteria for diagnosis of diseases of the heart and great vessels, 8th edition. Boston: Little, Brown and Co.; 1979:94.
17. Senda M, Tamaki N, Yonekura Y, et al. Performance characteristics of positologica. III. A whole-body positron emission tomograph. J Comput Assist Tomogr 1985;9:940-946.
18. Tamaki N, Yonekura Y, Yamashita K, et al. Value of rest-stress myocardial positron tomography using nitrogen-13-ammonia for the preoperative prediction of reversible asynergy. J Nucl Med 1989;30:1302-1310.
19. Tamaki N, Yonekura Y, Senda M, et al. Value and limitation of stress thallium-201 single-photon emission computed tomography: comparison with nitrogen-13-ammonia positron tomography. J Nucl Med 1988;29:1181-1188.
20. Tamaki N, Yonekura Y, Yamashita K, et al. Positron emission tomography using fluorine-18-deoxyglucose in evaluation of coronary artery bypass grafting. Am J Cardiol 1989;64:860-865.
21. Diamond GA, Forrester JS. Analysis of probability as an aid in the clinical diagnosis of coronary artery disease. N Engl J Med 1979;300:1350-1352.
22. Hoffman EJ, Huang SC, Phelps ME. Quantitation in positron emission computed tomography. I. Effect of object size. J Comput Assist Tomogr 1979;3:299-308.
23. Wisenberg G, Schelbert HR, Hoffman EJ, et al. In vivo quantification of myocardial blood flow by positron-emission computed tomography. Circulation 1981;63:1248-1258.
24. Parisi AF, Moynihan PF, Folland ED, Strauss WE, Sharma GVRK, Sasahara AA. Echocardiography in acute and remote myocardial infarction. Am J Cardiol 1980;46:1205-1214.
25. Matsuzaki M, Gallagher KP, Kemper WS, White F, Ross J Jr. Sustained regional dysfunction produced by prolonged coronary stenosis: gradual recovery after reperfusion. Circulation 1983;68:170-182.
26. Braunwald E, Kloner RA. The stunned myocardium: prolonged, postischemic ventricukar dysfunction. Circulation 1982;66:1146-1149.
27. Tamaki N, Yonekura Y, Yamashita K, et al. Relation of left ventricular perfusion and wall motion with metabolic activity in persistent defects on thallium-201 tomography in healed myocardial infarction. Am J Cardiol

1988;62:202-208.

28. Ratib O, Phelps ME, Huang SC, Henze E, Selin CE, Schelbert HR. Positron tomography with deoxyglucose for estimating local myocardial glucose metabolism. *J Nucl Med* 1982;23:577-586.

29. Yonekura Y, Tamaki N, Kambara H, et al. Detection of metabolic alterations in ischemic myocardium by F-18-fluorodeoxyglucose uptake with positron emission tomography. *Am J Cardiac Imaging* 1988;2:122-132.

30. Fudo T, Kambara H, Hashimoto T, et al. F-18-deoxyglucose and stress N-13-ammonia positron emission tomography in anterior wall healed myocardial infarction. *Am J Cardiol* 1988;61:1191-1197.

31. White CW, Wilson RF, Marcus ML. Methods of measuring myocardial blood flow in humans. *Prog Cardiovasc Dis* 1988;31:79-94.

32. Senda M, Yonekura Y, Tamaki N, et al. Interpolating and oblique-angle tomograms in myocardial PET using nitrogen-13-ammonia. *J Nucl Med* 1986;27:1830-1836.

SELF-STUDY TEST
Gastrointestinal Nuclear Medicine

Questions are taken from the *Nuclear Medicine Self-Study Program I*,
published by The Society of Nuclear Medicine

DIRECTIONS

The following items consist of a heading followed by lettered options related to that heading. Select the one lettered option that is best for each item. Answers may be found on page 718.

1. You are shown the gastric emptying time-activity curve (Fig. 1) of a 4-month-old child obtained after ingestion of 120 ml of milk containing 100 μCi of ^{99m}Tc-sulfur colloid. The child had frequent episodes of spitting up and poor weight gain. There was no history of surgery. Which *one* of the following is the best interpretation of this study?

A. delayed gastric emptying
B. abnormally rapid gastric emptying
C. incoordinated gastric contractions
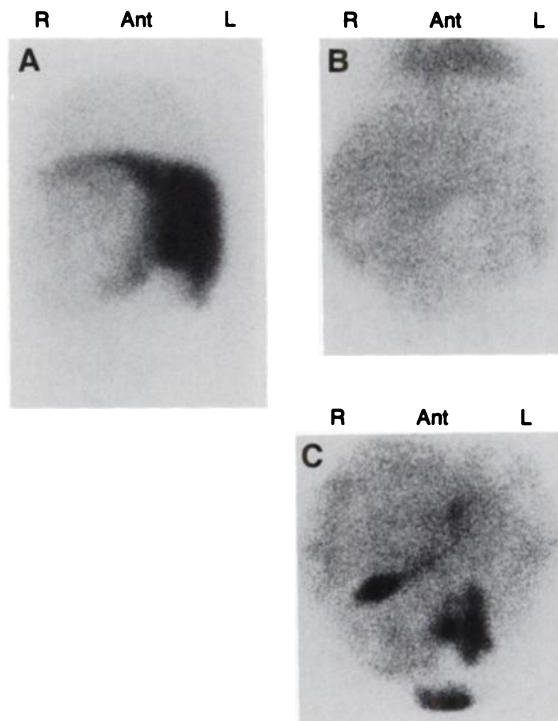D. artifactual abnormality
E. normal study

TIME
(MINUTES)
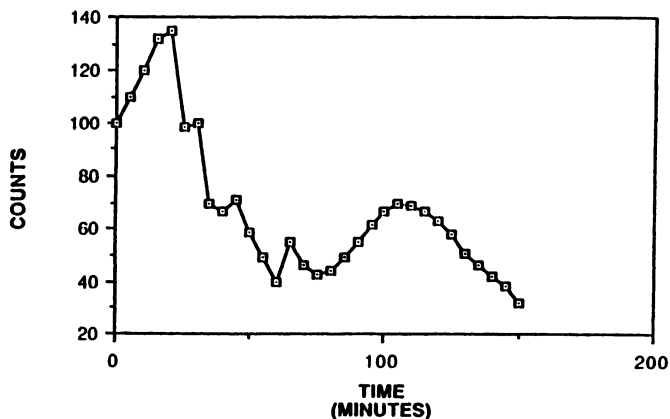
2. A 59-year-old man with a past history of treatment for tuberculosis developed muscle wasting, diarrhea, exertional dyspnea, abdominal swelling, and edema. A chest radiograph shows a normal size heart and a gated cardiac blood-pool study demonstrates a normal ejection fraction. There is no evidence for proteinuria. Because of hypoproteinemia, a ^{51}Cr-albumin study was ordered, which shows 15% of the administered dose excreted in the feces over a 4-day period. A barium study shows only mild edema of the small intestinal mucosa. Which *one* of the following is most likely to establish the diagnosis?

A. small bowel biopsy
B. cardiac catheterization
C. therapeutic trial of steroids

D. therapeutic trial with nonabsorbable antibiotics
E. therapeutic trial of a gluten-free diet

3. This 1-year-old boy has right upper quadrant fullness on physical examination. An anterior static view obtained with ^{99m}Tc-sulfur colloid (Fig. 2A), an anterior view of a ^{99m}Tc-labeled red cell study (Fig. 2B), and an image from a study with ^{99m}Tc-disofenin (Fig. 2C) are shown. Which *one* of the following is the most likely diagnosis?

A. cavernous hemangioma
B. focal nodular hyperplasia
C. congenital biliary ductal ectasia
D. metastatic neuroblastoma
E. hepatoblastoma

50 min